Photocatalytic Activity for NO Degradation by Construction Materials: Parametric Study and Multivariable Correlations

N. Bengtsson* and M. Castellote

Institute of Construction Science "Eduardo Torroja", CSIC, 28033 Madrid, Spain

Abstract:
Various standards have been published in an effort to rationalize and unify the evaluation and quantification of photocatalytic activity. The experimental conditions stated in the published standards and test methods differ in many aspects that make it very difficult to compare different results. This paper focuses on the influence of the different parameters involved in the photocatalytic process. The photocatalytic active material consists of white mortar, surface coated by TiO_2. The activity has been determined by quantifying the photocatalytic oxidation of NO. In the studied concentration interval the kinetics was estimated by a first order reaction. The influence on the activity by the relative humidity, temperature, irradiance, contaminant concentration and catalyst load has been studied. Most influent parameters are the catalyst load and light intensity until reaching plateau values at higher amount and intensity. Humidity influence the activity above 40% RH and an increased temperature lowers the activity. A global empirical correlation, including the mentioned variables, has been developed, allowing the determination of the photocatalytic activity at different environmental conditions (within the constraints of this research) and, when necessary, for comparison with reference conditions.

Keywords: Photocatalysis, NOx, construction materials, parametric study, kinetic constants, multivariable empirical correlation

Introduction

The photocatalytic activity of TiO_2 enriched building materials provides promising results for the degradation of air contaminates such as VOC (1-3) and NOx (4-7) performed in lab scale. Full scale studies proves that photocatalysis is effective also under real world conditions (8).

Differences in test methods and parameters cause difficulties in the comparison of photocatalytic activity of different materials. The unification of test methods requires a standardization of experimental procedures and conditions. Values for different parameters included in official standards and previous publications are compared in Table 1.

The differences between the compared parameters in Table 1 are the light source with difference in the wavelengths emitted and the intensity used in the measurements. The UVA intensity varies from 1.25 - 20 W/m^2. These values can be compared to the irradiance on a cloud free mid day in the middle of July in Madrid equal to 10 W/m^2 measured by a DelthaOhm 2102.1 radiometer with LP471 UVA sensor. The temperature and humidity are in the range of 20 to 27 °C and 50% RH conditions normally found in outdoor conditions. Continuous flow is used in the majority of the tests with gas flow rates of 1, 3 and 5 l/min. Initial NO concentration is in the range of 0.1 to 1 ppm and the UNI standard presents an initial mixture of both NO and NO_2.

Therefore, it is clear that the experimental conditions stated in the published standards and in literature differ in many aspects that make it very difficult to compare different results. Even though some research have been reported in the literature (5, 9-15, 20, 23, 25-27) on the influence of different parameters, a comprehensive parametric study and global correlation are needed in order to allow the estimation of the photocatalytic activity at different environmental conditions and, when necessary for comparison width reference conditions.

The aim of the presented paper is to determine the influence of the different experimental parameters involved in the photocatalytic degradation of NO on white mortar, coated with TiO_2. The influence of the following parameters has been evaluated: Temperature (T), relative humidity (RH), absolute humidity, irradiance (I), catalyst load (CL) and initial concentration (IC) of the studied compounds. These parameters, on the basis of the experimentally fitted kinetic constants, have been empirically correlated in a global relationship.

*Corresponding author; E-mail address: nicklas@ietcc.csic.es
Tel.: +34913020440, Fax: +34913020700

Table 1. Summary of experimental conditions presented in standards and previous publications for NOx abatement.

Standardization body/publication	ISO	JIS	UNI	[11]	[12]
Standard	22197-1	R 1701-1	11247		
Type of tests	Continuous flow	Continuous flow	Continuous flow	Batch	Continuous flow
Irradiation source	Fluorescent light BL or BLB; Xenon with filter letting pass (300 - 400 nm)	Fluorescent lamp (300 – 400 nm)	Osram Utravitalux	254/365 nm	300 – 400 nm
Irradiance (W/m^2)	10	10	20	(0.00125 - 0.00375), (0 - 0.1)	10
Temperature (ºC)	25	25	27		20
Relative humidity (%RH)	50	50	50	3 - 22 g/m^3	50
Gas flow (l/min)	3	3	5	-	1, 3 ,5
Initial concentration NO (ppm)	1	1	0.4		0.1, 0.3, 0.5, 1.0
Initial concentration NO_2 (ppm)	0	0	0.15		0
Size sample (cm^2)	50	50	65		171

Experimental Details

Materials

The following materials where used in the study. White cement type BL II/A-LL 52.5 N; Degussa P25 as the active photocatalyst; Liquid silicone; Air with an O_2 concentration of 20% in N_2, with purity above 99.999%; NO 4.6 ppmvol, balanced by N_2 width relative uncertainty of the measurement: ± 5%.

Methods

Sample Preparation

White mortar was prepared in petri dishes with a diameter of 90 mm and a height of 16 mm, using white cement type BL II/A-LL 52.5 N with the following ratios: cement/sand: 0.33 and water/cement: 0.5. The fresh mortar was cured for 28 days at >95% RH and 23 ±2 °C.

Liquid silicone was applied on the border of the top surface of the sample, surrounding a circular area of 50.2 cm^2. A colloidal suspension of TiO_2 in deionised water with a concentration of 8.37 (g/l) was applied on the surface of the mortar surrounded by silicone. A total volume of 3 ml was added to give a final TiO_2 mass load of 5 g/m^2 after evaporation of the water in the suspension at room temperature. The resulting TiO_2 layers were examined by BSE. They were compact layers of around 10 µm, as it can be seen in Figure 1. The samples were stored at 50% RH and 20 °C at least 48 hours prior to the tests. At the border between silicone and TiO_2 some interference is possible, but due to the small amount of TiO_2 in contact with silicone compared to the total amount of TiO_2 covering the surface, the possible influence has been neglected.

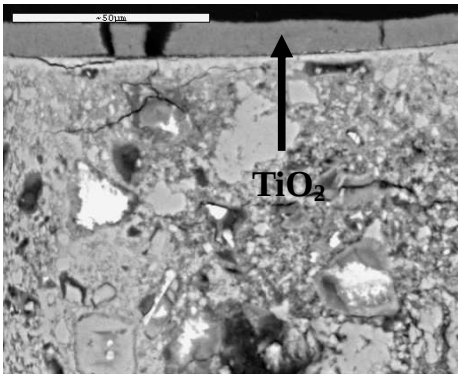

Figure 1. BSE image of the surface of one sample of mortar.

Photocatalytic Reactor and Experimental Procedure

The reactor was designed according to the standard ISO 22197-1 (16) with some modifications: The width of the gas flow channel was 112 mm and the distance between sample and window 4 mm. The interior of the reactor in contact with the airflow was made of glass and the window for UV entrance was made of Pyrex. The experiments were also performed according to the mentioned standard, with the exception that the gas flow was recycled by an airtight pump with a recycling flow rate of 5.2 l/min. Two containers were connected in the recirculation loop to achieve a total volume of the setup of 56 liters. The irradiation was performed by 2 Philips Actinic BL 15W/10 SLV fluorescent tubes emitting irradiance in UVA radiation at an optimum of 365 nm.

The initial NO concentration in the system was controlled by adjusting the inlet flow by Brooks flow

Table 2. Experimental parameters for the NOx oxidation tests.

Test	Temperature (ºC)	Humidity (%RH)	Absolute humidity (g/m^3)	Irradiance (W/m^2)	Catalyst load (g/m^2)	Initial NO concentration (ppbv)	Initial NO_2 concentration (ppbv)
N1	21	62	9.5	10	5.0	964	34
N2	26	42	8.5	10	5.0	1000	51
N3	30	42	10.8	10	5.0	899	25
N4	21	3.0	0	10	5.0	1050	37
N5	21	31	4.5	10	5.0	998	38
N6	22	37	6.5	10	5.0	1030	51
N7	21	65	10	10	5.0	982	50
N8	21	60	9.2	0.5	5.0	985	49
N9	21	59	9.0	1	5.0	996	51
N10	21	59	9.0	2.5	5.0	972	62
N11	21	60	9.0	5	5.0	981	49
N12	21	63	9.5	18	5.0	1010	75
N13	22	57	9.5	10	2.5	976	69
N14	22	60	10	10	10	964	78
N15	21	60	9.0	10	5.0	101	11
N16	20	68	9.8	10	5.0	393	16
N17	21	65	8.5	10	5.0	675	27
N18	21	58	9.0	10	0	1000	77
N19	21	58	9.0	0	5.0	991	66

controllers giving a resulting gas mixture of air and NO/N_2, that was let to stabilize until obtaining a concentration of 1000 ppb. The humidity was set by passing a part of the airflow through a flask medium filled with water. The temperature was that of the ambient air in the laboratory.

The NO and NO_2 concentrations were measured simultaneously by AC32M (Enironmental S.A.) analyzing by Chemiluminiscence. The volume of the sample was of 0.66 liters and the concentration was measured just before the illumination was switched on, 15, 30, 45, 60, 90 and 120 minutes after the illumination was turned on.

The NO_3^- content, resulting from the mineralization of the NO, was analyzed by submerging the sample, after the experiment, in 50 ml deionized water for the elution of the NO_3^- formed on its surface.

Experimental Design

The influence of the parameters investigated in this paper was studied by vary them one by one, keeping the rest of the parameters constant. A summary of the parameter conditions used can be seen in Table 2. The test series are denoted with the abbreviations N1 to N19.

Each sample was tested once to preventing the use of a catalyst that has been deactivated by intermediates or initial compounds on the active sites.

Analysis of the Results

Two possible photocatalytic oxidation mechanisms for NO are reported in the literature. The most common proposes are an initial oxidation to NO_2 and then further oxidation to HNO_3 by the hydroxyl attack, generated by the activated photocatalyst. The alternative is an interaction by O_2^- to form NO_3^- (17).

The global process of a gas phase heterogeneous photocatalytic oxidation can be divided in 5 mayor intermediate steps (18):

1. Transfer of the reactants in the fluid phase to the surface
2. Adsorption of at least one of the reactants
3. Reaction in the adsorbed phase
4. Desorption of the product(s)
5. Removal of the products from the interface region

Taking into account all the steps would result in non affordable problem and the fact that the rate of the different steps normally is quite different and the slowest one is the rate limiting step that determines the rate of the global process. In the analysis of the kinetic data, some of these steps are often neglected.

The Langmuir-Hinshelwood (L-H) model Equation 1 is frequently used in the literature to model heterogeneous solid-gas phase reactions (17, 19). The model includes the saturation of the active sites by the

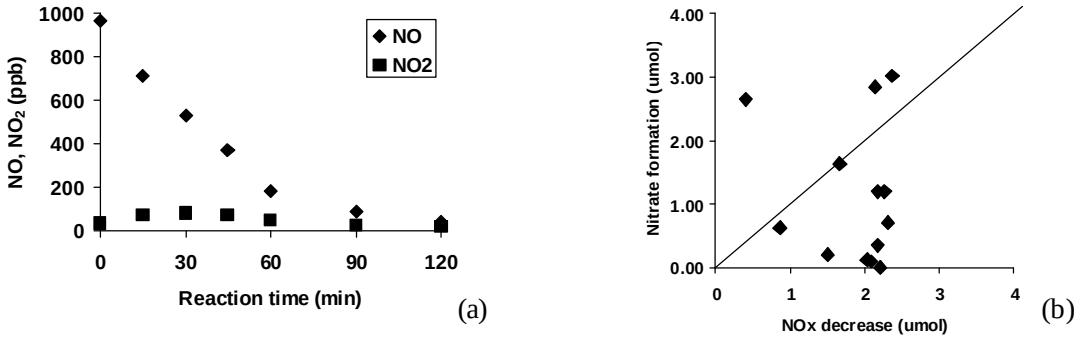

Figure 2. (a) Illustration of NO oxidation and NO_2 formation over time under UV irradiation. Values taken from test N1. (b) Nitrate formation as a function of the NOx concentration decrease.

adsorption-desorption equilibrium of the substrate (intermediate steps 2, 3 and 4).

$$\frac{dC}{dt} = -\frac{kKC}{1+KC} \quad (1)$$

where C is the concentration of NO (ppb), k is the reaction constant (min^{-1}) and K is the binding constant for NO on the active site. The determination of the reaction constant k and the Langmuir adsorption constant K is done by inversion of Equation 1 and plotting $1/r_0$ as a function of $1/C_0$ Equation 2 (19).

$$\frac{1}{r_0} = -\frac{1}{kK}\frac{1}{C_0} + \frac{1}{k} \quad (2)$$

where r_0 is the initial reaction rate during the first 15 minutes and C_0 is the initial concentration. The literature presents important advances in the kinetics of photocatalytic reactions mainly concerned the development of specific models based on the L-H equations. A summary of variations of the L-H models is given by G. Li Puma et al. (20). The L-H model can be varied to take in account the adsorption of water vapor by a bimolecular model of single site competitive, two site non competitive and two sites competitive. Hunger et al. presents a L-H mechanism, including the three components NO, NO_2 and H_2O (21).

Provided that the kinetic model is dependent not only on the catalyst but also on the contaminant, in this study, the analysis of the results have been carried out in the following steps: 1) confirmation of the degradation pathway; 2) search of the controlling step in the global reaction process with the analysis of the mass transport influence, and 3) modeling of the rate of the reaction starting with the monomolecular L-H model Equation 1.

Results and Discussion

Degradation Pathway

Under UV radiation a decrease in NO concentration over time was determined with a simultaneous formation and later degradation of the intermediate NO_2, Figure 2-a. It can be seen that after 120 minutes of radiation almost complete degradation of both NO and NO_2 is detected. In Figure 2b, the amount of NO_3^- formed in relation to the gas phase decrease of NOx in the system are depicted. Even though there is not a linear relationship (which has been attributed to the bias in the analysis of NO_3^- due to the very low concentrations), the mineralization to NO_3^- is demonstrated according to the oxidation pathway Equation 3.

$$NO \rightarrow NO_2 \rightarrow NO_3^- \quad (3)$$

Reaction Model: Controlling Step

Influence of the Transfer Matter (steps 1 and 5)

The experimental setup acts as a CST tank, in line with similar setups in previous publication (22). However concerning the mass transport inside the reactor the gas does have a slit flow characteristics and the low Reynolds number of 97 assuming a laminar double-skin photoreactor.

The confirmation that the diffusion is not the rate limiting step is proved according to the method described by Hunger et al. (21). The assumption is described below.

Assume that the reaction on the surface is instantaneous; meaning that C_w is equal to zero, that would result in that the mass transport is the limiting step. The mass flux of NO by diffusion from the gas to surface is governed by Equation 4:

$$m = \frac{ShD}{d_h}(C_g - C_w) = \frac{ShD}{2h}(C_g - C_w) \quad (4)$$

where: m is the mass flux of NO, Sh is the Sherwood number, D the diffusion coefficient (m^2/s), d_h the hydraulic diameter, C_g the NO concentration, the mean mixed or bulk in gaseous phase, C_w the NO concentration on the surface, h the height (m). The values for the constants art taken from (21) with Sh amount to

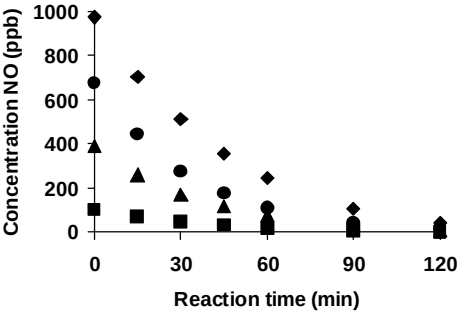

Figure 3. Photocatalytic NO oxidation over time at different initial concentrations.

about 5 and D estimated to $1.51 \cdot 10^{-5}$ m^2/s. The gas velocity is 0.19 m/s and de and h = 4 mm.

The boundary condition is:

$$C_g = C_{g,in} \tag{5}$$

Giving as integrated form

$$\frac{C_{g,out}}{C_{g,in}} = e^{-\frac{ShDL}{2v_{air}h^2}} = e^{-\frac{5 \cdot 1.5 \cdot 10^{-5} \cdot 0.08}{2 \cdot 0.19 \cdot 0.004^2}} = 0.37 \tag{6}$$

where L is the length of the sample, set to 8 cm due to its circular shape and V_{air} the velocity of the gas over the sample surface. This result signify a 63% NO degradation. The time it takes for the whole gas volume in the experimental set up to pass the reactor is little bit more than 10 minutes. If the mass transfer is the rate limiting step a degradation of NO after the mentioned time would be 63% that is far higher than the degradation results after 10 minutes in this study. This fact demonstrates that the diffusion is not the rate limiting step. The C_W is now equal to C_g.

Therefore, according to the global reaction model, the reaction rate can be limited by the intermediate steps (2, 3 and 4) and then, the Langmuir-Hinshelwood (L-H) model will be tried.

Influence of the Adsorption/Desorption (steps 2 and 4)

The NO oxidation over time varying the initial concentration of NO is illustrated in Figure 3. In all cases an almost complete disappearance of NO is seen after 120 minutes of reaction.

The initial reaction rates (r_0) estimated by the decrease in NO concentration during the first 15 minutes as a function of the different initial concentrations (C_0) demonstrate a linear relation normally seen at low concentration in the L-H model, Figure 4a.

From the good linearity of $1/r_0$ as a function of $1/C_0$ and intercept of the linear regression on the y-axis

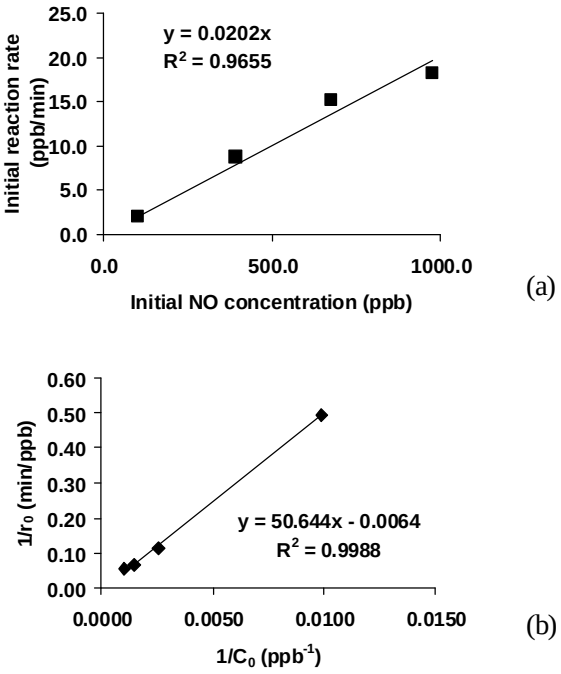

Figure 4. (a) Initial reaction rate as a function of initial concentration. (b) $1/r_0$ as a function of $1/C_0$.

very close to zero, Figure 4b. The small intercept value gives a very small K value with a minor influence on the L-H mechanism and is therefore neglected. The resulting equation is a first order reaction. The lack of influence of the adsorption/desorption equilibrium concludes that step 3 in the global heterogeneous reaction is the rate limiting step.

Estimation of the Order of the Reaction (step 3)

The first order reaction model is given in Equation 7 and integrated in Equation 8. The model fitting and estimation of the reaction rate is illustrated in Figure 5, where it can be deduced that there is a good fit to the experimental results and therefore, the reaction rate constant obtained form each test is used to compare the influence of the parameters studied in this work.

$$\frac{dC}{dt} = -k_{NO} C \tag{7}$$

$$\ln\left(\frac{C_0}{C}\right) = k_{NO} \cdot t \tag{8}$$

where: C_0 is the initial NO concentration (ppb) t, the time (min) and k_{NO} the reaction rate constant (min^{-1}).

Parametric Study

Influence of the Irradiance

The NO degradation rate influenced by the irradiance is increasing until reaching a plateau above 5

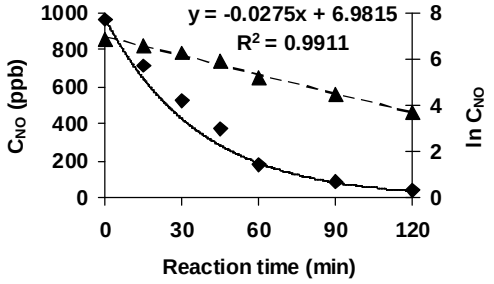

Figure 5. Model adjustments (straight line) to the experimental data (diamonds), ln C_{NO} (triangles) and linear adjustment (dashed line) for test N1.

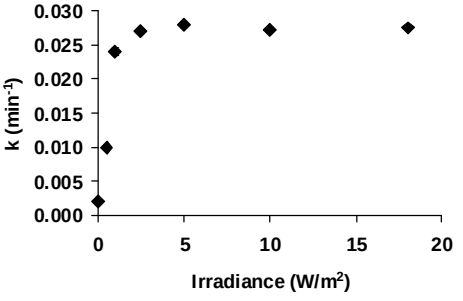

Figure 6. Influence of the light intensity (tests N1, N8-N12, N19) in the NO oxidation rate.

W/m^2. The irradiance interval can be divided into two parts. At lower intensities from 0 to 1 W/m^2 the influence on the reaction rate constant demonstrates a linear relation. At light intensities above 1 W/m^2 the increase follows a square root relation, Figure 6. The division of the influence of irradiance in two segments, one linear at lower intensities and proportional to I^n, where $0.5 < n < 1$ has previously been mentioned (23). A similar relation has been demonstrated for isopropanol degradation following a linear relation at low intensity until reaching a square root relation (0.5) above one sun equivalent (24). The difference in irradiance dependency is described by Chen et al. explaining the phenomena by the fact that at lower radiation intensities the chemical reaction is faster than the recombination rate of the electrons and holes. On the other hand when the irradiance is increased the recombination of electrons and holes becomes the dominant process that negatively influences the activity (9).

The formal quantum efficiency (FQE) Equation 9, mentioned in a previous publication (23) is calculated instead of the quantum yield that is difficult to determine due to the fact that incident light may be absorbed, reflected or scattered.

$$\delta = \frac{rate\ of\ \ photocatalyzed\ reactions\ (molecules/s)}{incident\ light\ \text{int}ensity\ (photons/s)} \quad (9)$$

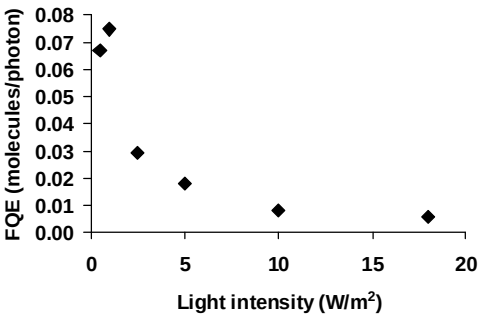

Figure 7. Formal quantum efficiency as function of light intensity.

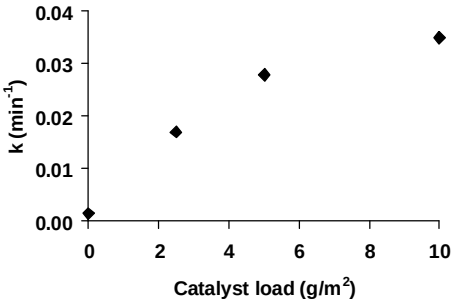

Figure 8. Initial NO oxidation rate by the influence of the catalyst load on the surface of the sample (test N1, N13, N14, N18).

The FQE as a function of the light intensity gives a maximum of 0.07 molecules per photon at a light intensity of 1 W/m^2 (Figure 7) that can be compared to previous values ranging from 0.0006 to 0.12 summarized by Chin et al (23).

Influence of Catalyst Load

By increasing the mass load of TiO_2, a higher reaction rate constant for the NO oxidation was observed, Figure 8. The influence of the mass load on the reaction rate constant follows a non linear behavior according to the adjustment presented by Lewandowski et al. (27). This equation was modified to fit the reaction constants as a function of the mass load of catalyst, Equation 10. The equation gives a good estimation of the experimental data in this study with $\alpha = 0.31$ and $k_{max} = 0.035$. In the lower concentration range the catalysts load is a factor with an important influence, but when increasing the load above 5g/m^2 the influence of the mass load becomes less predominant. Results presented by Toma et al. (10) demonstrate that depending on the size of the sample a TiO_2 mass load above 15 or 30 g/m^2 does not further enhance the photocatalytic activity. Puzenat (11) explain the phenomena by the fact that the maximum amount of TiO_2 totally illuminated is reached. Li Puma et al give a similar explanation stating that in thick films there is not an effective radiation of all the catalyst, having the surface

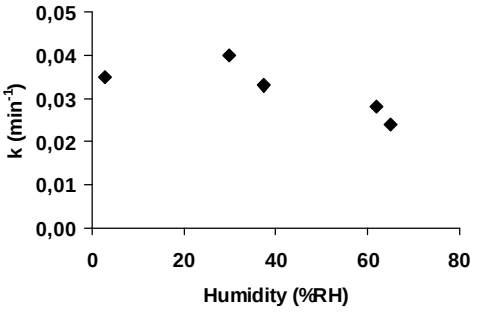

Figure 9. Initial NO oxidation rate constant as a function of the humidity (tests N1, N4-N7).

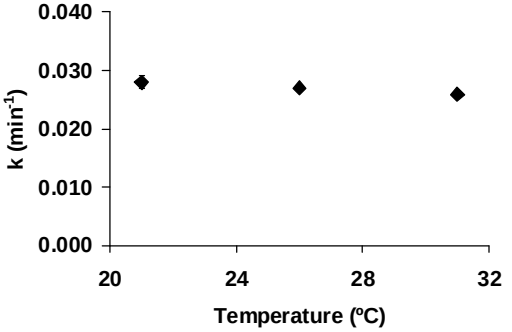

Figure 10. Initial NO oxidation rate by the influence of the temperature maintaining the absolute humidity constant (tests N1-N3).

catalyst illuminated but the interior catalyst inactive. (20).

$$k_{NO} = k_{NO,\max}(1 - e^{-\alpha \cdot CL}) \qquad (10)$$

where α is a constant.

The thickness of the TiO_2 coating was measured to be around 10 μm at a mass load of 5g/m^2 by BSE microscopy, Figure 1. Having in mind that the critical mass is not reached the coating is thicker than previous published results mentioning a critical thickness of 2 μm (25) and 350 nm (20).

Influence of Humidity

Photocatalytic activity was observed at almost zero humidity and the activity does not change remarkably until reaching humidity levels above 40% RH where a decrease in the reaction rate was noticed, Figure 9. Hüsken et al. reported a negative effect of the humidity on the NO degradation rate with a linear decrease of the activity by increased humidity in the range 10 – 80% RH due to competitive adsorption between water and contaminant on the active sites (5).

Chen et al. presented an optimum in the reaction rate of NOx abatement at 25% RH and 25 °C by injecting the pollutant after adjusting the humidity in the reactor. The optimum of the rate constant was explained by the formation of free OH radicals promoting the oxidation until a certain extent before competitive adsorption of NO and the water molecules take place on the active sites at higher humidity levels (9).

The influence of the adsorption of water was confirmed by Sauer et al. (22), proving that when raising the humidity more water is adsorbed on the TiO_2 surface, leading to the decrease of the adsorption of substrates.

The influence of the humidity on the photocatalytic activity depends on the type of compound studied. The humidity inhibits the conversion of formaldehyde (12), isopropanol, trichloroethylene and acetone, but enhances toluene oxidation and has no significant effect on 1-butanol. M-xylene oxidation is increased by the humidity up to 1500 mg/m^3 and decrease at higher values (13). Amama et al. (14) studied the gas phase degradation of trichloroethylene (TCE) in the range of 0 to 100% RH, with the conclusion that the TCE mineralization was highest in the range 50 – 100% RH.

The difference in the influence of the humidity is related to interactions between water and intermediates (14) and the hydrophilic properties of the surface of the active material (26).

Influence of Temperature

An increase in temperature slightly decreases the reaction rate constant, Figure 10. According to the literature the temperature influences the activity by affecting the adsorption and desorption rate constants (27).

Influence of the Contaminant Concentration

The reaction rate constant does not change when the initial NO concentration is altered verifying the conclusion that the reaction rate is of first order reaction in the studied concentration interval, see Figure 11.

Multiple Parameter Fitting of the Photocatalytic Activity

Until now, the kinetic constants calculated are related to the variation of a single parameter maintaining the rest of them constant. Therefore, in order to find a global correlation able to be applied at different conditions for every parameter (in the range studied in this work), non linear estimation has been tried, including every variable analyzed, for the kinetic constants of the degradation of NO, including all the matrix of data corresponding to every test performed.

The best empirical correlation found, Equation 11 for the oxidation of NO, includes 4 variables: temperature (T) in degrees Celsius, relative humidity (RH)

Table 3. Numeric values for the fitting constants for the multiple parameter equation 13.

a1	b1	c1	d1	h1	j1	m1	n1
-4.59	-0.0658	4.55	-0.000662	0.0189	0.166	0.0141	0.419
Ranges of validity : 21 < T(ºC) < 30; 3 < RH < 56; 0 < I < 18; 0 < CL < 10; 101 < IC (NO) < 964							

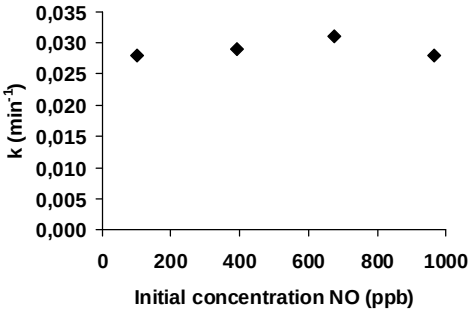

Figure 11. NO oxidation rate constant by the influence of the initial concentration of NO (tests N1, N15-N17).

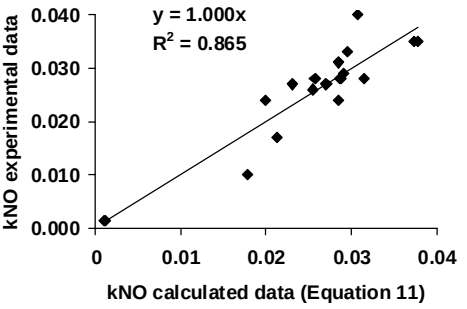

Figure 12. Comparison of the experimental values of de-contamination of NO and values for the global correlation obtained through Equation 11.

in %RH, irradiance (I) in W/m^2 and catalyst load (CL) in g/m^2, explaining a variance of the 86.5% of the data.

$$k_{NO} = a1 \cdot e^{(b1/T)} + c1 \cdot RH^{d1} + h1 \cdot I^{j1} + m1 \cdot CL^{n1} \quad (11)$$

where a1, b1, c1, d1, h1, j1, m1 and n1 are the fitting parameters given in Table 3 where the range of validity of the equation for each parameter is also given.

By application of the obtained k_{NO} Equation 11, in equations 7 and 8, the kinetics of degradation of NO in any experimental condition (within the constrains of this study) can be obtained.

The absolute humidity depends on the T and RH, therefore it is not included in the correlation. The initial concentration (IC) is not included in the fit due to absence of influence on the reaction constant k in the studied interval, demonstrated in Figure 11.

Figure 12 illustrates the comparison between the experimental values and the calculated values obtained through Equation. 11, for $k_{NO.}$ From Figure 12 it can be deduced that, within the ranges included in this study, the correlations are good enough to be used to predict the photocatalytic degradation in different conditions.

Conclusions

In this paper a parametric study, in function of the kinetic constants, on the influence of the key variables in the photocatalytic activity of oxidation of NO has been carried out. The variables included in the study are the relative humidity, temperature, irradiance, contaminant concentration and catalyst load, and the following conclusions have been done:

- The reaction kinetics of the NO oxidation has been established, proving an elemental first order reaction.
- The parameters studied in this work influence the activity of the photocatalytic NO oxidation according to the following conclusions.
- For the studied intervals, the NO oxidation is approaching a plateau value at a catalyst load of 10 g/m^2 and a plateau is found above an irradiance of 5 W/m^2, concluding that at above a certain level of irradiance and catalyst load their influence does not affect the reaction rate.
- No influence of the humidity was noticed on NO oxidation in the range form 3 to 40% RH, however above 40% RH a decrease in activity was observed, which could be attributed to the competitive adsorption of water and the contaminant on the active sites of the catalyst.
- An increase in temperature while maintaining the absolute humidity constant resulted in a decrease in the activity for NO oxidation.
- The absence of influence by the initial concentration of NO on the reaction rate constant proves that the reaction follows a first order in the studied concentration range.
- A global empirical correlation, including the studied variables has been proposed, allowing the estimation of the photocatalytic activity at different environmental conditions, including for reference conditions for comparison.

Acknowledgments

The authors would like to thank the Spanish Ministry of Science and Innovation for the financial support of this project.

References

(1) Stirini, A.; Cassese, L.; Schiavi, L. *Applied Catalysis B: Environmental* **2005**, *61*, 90-97.

(2) Demeestere, K.; Dewulf, J.; Witte, B. D.; Baeldens, A.; Langenhove, H. V. *Building and Environment* **2008**, *43*, 406-414.

(3) Maury, A.; Demeestere, K.; De Belie, N.; Mäntylä, T.; Levänen, E. *Building and Environment* **2010**, *45*, 832-838.

(4) Cassar, L. *Materials Research Society* **2004**, *29*(5), 328-331.

(5) Hüsken, G.; Hunger, M.; Brouwers, H.J.H. *Building and Environment* **2009**, *44*, 2463-2474.

(6) Chen, J.; Poon, C. *Building and Environment* **2009**, *44*, 1899-1906.

(7) Bengtsson, N.; Castellote, M.; López-Muñoz, M. Cerro, L. *J. Adv. Oxid. Technol.* **2009**, *1*, 55-63.

(8) Maggos T.; Bartizis J. G. Liakou, M.; Gobin, C. *Journal of Hazardous Materials* **2007**, *146*, 668-673.

(9) Chen, M.; Yan, L. *Journal of Hazardous Materials* **2010**, *174*, 375-379.

(10) Toma, F.; Guessasma, S,; Klein, D.; Montavon, G.; Bertrand, G.; Coddet, C. *Journal of Photochemistry and Photobiology A: Chemistry* **2004**, *165*, 91-96.

(11) Puzenat, E. *The European Physical Journal Conferences* **2009**, *1*, 69-74.

(12) Ao, C.H.; Lee, S.C.; Yu, J.Z.; Xu, J.H. *Applied Catalysis B: Environmental* **2004**, *54*, 41-50.

(13) Luo, Y.; Ollis, D. *Journal of Catalysis* **1996**, *163*, 1-11.

(14) Amama, P. B.; Itoh, K.; Murabayashi, M. *Journal of Molecular Catalysis A Chemical* **2004**, *217*, 109-115.

(15) Kakinoki, K.; Yamane, K.; Teraoka, R.; Otsuka, M.; Matsuda, Y. *Journal of Pharmaceutical Sciences* **2003**, *93*, 582-589.

(16) ISO 22197-1, Fine ceramics (advanced ceramics, advanced technical ceramics) Test methods for air purification performance of semiconductor photocatalytic materials. Part 1: Removal of nitric oxide, first ed., 2007.

(17) Ballari, M. M..; Hunger, M.; Hüsken, G.; Brouwers, H. J. H. *Applied Catalysis B: Environmental* **2010**.

(18) Pichat, P.; Herrmann, J. M. *Photocatalysis Fundamentals and Applications*; John Wiley and sons: 1989, chapter 8, 217-250.

(19) Kim, S. B.; Hong, S. C. *Applied Catalysis B: Environmental* **2002**, *35*, 305-315.

(20) Puma, G. L.; Salvadó-Estivill, I.; Obee, T. N.; Hay, S. O. *Separation and Purification Technology* **2009**, *67*, 226-232.

(21) Hunger, M.; Brouwers, H. J. H.; Ballari, M. In *1st international Conference on Microstructure Relating Durability of Cementous Composites*; 2008, pp 1103-1112.

(22) Sauer, M. L.; Ollis, D. F. *Journal of Catalysis* **1994**, *149*, 81-91.

(23) Chin, P.; Yang, L. P.; Ollis, D. F. *Journal of Catalysis* **2006**, *237*, 29-37.

(24) Ollis, D.F. *Comptes Rendus de l'Académie des Sciences - Series IIC - Chemistry* **2000**, *3*, 405-411.

(25) Childs, L. P.; Ollis, D. F. *Journal of Catalysis* **1980**, *66*, 383-390.

(26) Wang, K.; Tsai, H.; Hsieh, Y. *Applied Catalysis B: Environmental* **1998**, *17*, 313-320.

(27) Lewandowski, M.; Ollis, D. F. *Applied Catalysis B; Environmental* **2003**, *43*, 309-327.

Received for review February 1, 2010. Revised manuscript received March 20, 2010. Accepted March 21, 2010.